Nitrogen chemistry controlling steps in methane–air premixed flames

Dimitris A. Goussis*, George Skevis

Institute of Chemical Engineering and High Chemical Processes, FORTH/ICE-HT, Stadiou Street, 26500 Rio, Patra, Greece

Abstract

The important kinetics paths for NO_x formation and the dynamics for their equilibration in a premixed methane–air flame are analyzed with tools from CSP. It is shown that controlling components of well-known paths (i.e. prompt, thermal, nitrous) are associated with the slowest time scales of the process. The details of their transition along the flame from active to equilibrated status provide significant physical understanding.

Keywords: Flames; Combustion; NO_x formation; Inertial manifolds; Stiff ODEs

1. Introduction

Environmental and energy efficiency needs demand the ability to accurately simulate and physically understand complex combustion processes. Such efforts produced well-established efficient solvers and elaborate chemical kinetics mechanisms. The need for physical understanding is currently addressed by different methods (such as reaction path analysis, sensitivity, asymptotic methods, etc.). However, the complexity of the mathematical models and kinetic mechanisms employed by both research and industry, render these methods difficult to use. The availability of numerical algorithms that can produce directly the physical understanding needed, would greatly enhance our ability to analyze reacting flows.

Here it will be demonstrated that the Computational Singular Perturbation (CSP) method [1,2] can be employed for such a purpose, by analyzing a steady premixed methane–air flame. The analysis will concentrate on the evolution of the nitrogen chemistry across the flame and on its interaction with the carbon chemistry and the oxy-hydrogen pool. More attention will be given to the related slowest chemical time scales, which are associated to the controlling paths for NO_x formation. Next, a brief presentation of CSP will be given, as it applies to the analysis of reacting flows, and then results will be presented and discussed.

* Corresponding author. Tel.: +30 2610 965251; Fax: +30 2610 965223; E-mail: dagoussi@iceht.forth.gr

2. CSP tools

Given a detailed kinetic mechanism consisting of N species, E elements and K elementary reactions (forward and backward directions counted separately), the species conservation steady state equation in N-dimensional vector form is:

$$0 = \mathbf{L}_c(\mathbf{y}) + \mathbf{L}_d(\mathbf{y}) + \frac{1}{\rho}\mathbf{W}\left[\mathbf{S}_1 F^1(\mathbf{y}) + ... + \mathbf{S}_K F^K(\mathbf{y})\right] \quad (1)$$

where, $\mathbf{y}$ is the vector of the species mass fractions, $\mathbf{L}_c$ and $\mathbf{L}_d$ are the convective and diffusive differential vector operators, ρ is the mixture density, $\mathbf{W}$ is a matrix with the molecular weights in the diagonal, $\mathbf{S}_k$ is the stoichiometric vector of the k-th elementary reaction and F^k is the corresponding reaction rate. Equation (1) is cast as:

$$0 = \mathbf{a}_1 h^1 + ... + \mathbf{a}_N h^N \quad (2)$$

where

$$h^i = \mathbf{b}^i \mathbf{L}_c(\mathbf{y}) + \mathbf{b}^i \mathbf{L}_d(\mathbf{y}) + \frac{1}{\rho} f^i \quad (3a)$$

$$\mathbf{b}^i \mathbf{L}_c(\mathbf{y}) = b_1^i L_c^1 + ... + b_N^i L_c^N \quad (3b)$$

$$\mathbf{b}^i \mathbf{L}_d(\mathbf{y}) = b_1^i L_d^1 + ... + b_N^i L_d^N \quad (3c)$$

$$f^i = \mathbf{b}^i \mathbf{W} \mathbf{S}_1 F^1 + ... + \mathbf{b}^i \mathbf{W} \mathbf{S}_K F^K \quad (3d)$$

the column vectors $\mathbf{a}_i$ and row vectors $\mathbf{b}^i$ are the CSP basis vectors and their dual ($\mathbf{b}^i \mathbf{a}_k = \delta_k^i$); b_n^i, L_c^n and L_d^n

are the n-th elements of the $\mathbf{b}^i$ vector and the $\mathbf{L}_c$ and $\mathbf{L}_d$ operators, respectively [1,2]. Each additive term in the RHS of Eq. (2) is defined as a mode, involving the product of a vector ($\mathbf{a}_i$) and an amplitude (h^i). They are ordered according to the chemical time scale they relate to; the $i = 1$ mode relates to the fastest scale $\tau_{chem,1}$, etc. Due to the conservation of the E elements in all $\mathbf{S}_k$'s, the last CSP $\mathbf{b}^i$ vectors ($i = N - E + 1, N$) yield $\mathbf{b}^i \mathbf{WS}_k \equiv 0$, so that $\tau_{chem,i} = \infty$ and $f^i = 0$; i.e. the last E h^i's are independent of chemical kinetics.

Since the vectors $\mathbf{a}_i$ are linearly independent, Eq. (2) yields $h^i \equiv 0$ ($i = 1, N$). As shown by Eqs. (3a–d), the expressions $h^i \equiv 0$ are established due to cancellations among the K chemical and 2N transport terms. The nature of the dominant cancellations in each expression $h^i \equiv 0$, points to the major physical processes involved. In order to estimate the action of the different convective, diffusive and chemical terms in $h^i \equiv 0$ we introduce the indices:

$$I_c^i = \sum_{n=1,N} \left| \frac{b_n^i L_c^n}{Q} \right| \quad I_d^i = \sum_{n=1,N} \left| \frac{b_n^i L_d^n}{Q} \right| \quad I_s^i = \sum_{k=1,K} \left| \frac{\mathbf{b}^i \mathbf{WS}_k F^k}{\rho Q} \right|$$

$$(4a - c)$$

where

$$Q = \sum_{n=1,N} \left| b_n^i L_c^n \right| + \sum_{n=1,N} \left| b_n^i L_d^n \right| + \sum_{k=1,K} \left| \frac{\mathbf{b}^i \mathbf{WS}_k F^k}{\rho} \right|$$

Since $I_c^i + I_d^i + I_s^i = 1$, values of I_c^i, I_d^i or I_s^i close to unity indicate dominance of convection, diffusion or chemistry, respectively, in h^i.

Here, the CSP vectors $\mathbf{a}_i$ and $\mathbf{b}^i$ are approximated by their leading order term: the right and left, respectively, eigenvectors of the Jacobian of the source term in Eq. (1). The chemical time scales are thus defined as $\tau_{chem,i} = 1/|\lambda_i|$, where λ_i is the i-th eigenvalue acting along the direction $\mathbf{a}_i$ [2]. The eigenvalue λ_i is related to the K elementary reactions by the equation:

$$\lambda_i = \mathbf{b}^i \mathbf{WS}_1 \mathbf{G}^1 \mathbf{a}_i + \mathbf{b}^i \mathbf{WS}_2 \mathbf{G}^2 \mathbf{a}_i + \ldots + \mathbf{b}^i \mathbf{WS}_K \mathbf{G}^K \mathbf{a}_i \quad (5)$$

where $\mathbf{G}^k = \left[\partial/\partial y^1, \ldots, \partial/\partial y^N \right] \left(R^k/\rho \right)$. In order to assess the contribution of each elementary reaction to the value of λ_i, the following index is introduced:

$$\mathbf{J}_k^i = \frac{\mathbf{b}^i \mathbf{WS}_k \mathbf{G}^k \mathbf{a}_i}{|\mathbf{b}^i \mathbf{WS}_1 \mathbf{G}^1 \mathbf{a}_i| + \ldots + |\mathbf{b}^i \mathbf{WS}_K \mathbf{G}^K \mathbf{a}_i|} \quad (6)$$

where $|J_1^i| + |J_2^i| + \ldots + |J_K^i| = 1$. Since negative (positive) values of λ_i indicate a drive of the i-th CSP mode towards (away from) equilibrium, i.e. $h^i \equiv 0$, similarly negative (positive) values of $\mathbf{J}_K^i$ indicate action of the k-th elementary reaction towards (away from) equilibrium.

The species most affected by each $\tau_{chem,i}$ and chemical

component of $h^i \equiv 0$ (known as CSP radicals) is identified by the CSP pointer [2].

3. Flame structure

A steady, 1-D freely propagating, adiabatic, laminar, stoichiomeric, premixed atmospheric $CH_4/O_2/N_2$ flame was computed using the RUN-1DL code [3] and the GRI-3.0 detailed mechanism, incorporating 53 species (N = 53), 325 reversible reactions (K = 650) and 5 elements (E = 5) [4]. The profiles of temperature and of selected nitrogen compounds are shown in Figs. 1 and 2.

For this process it is well known that upstream of the flame the only physical mechanism active is transport, while downstream chemical equilibrium determines completely the state [5]. The transition from transport to
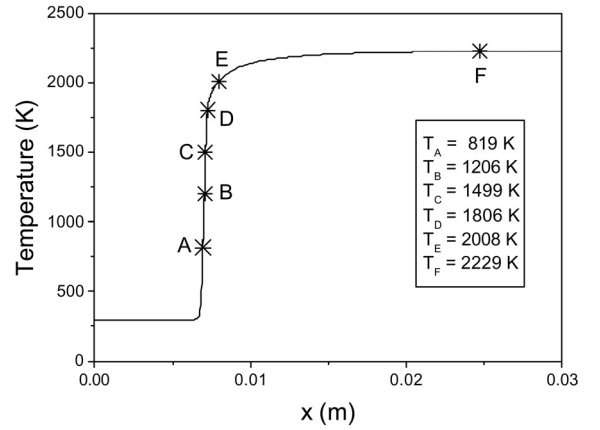

Fig. 1. Temperature profile in the stoichiometric premixed methane–air flame.
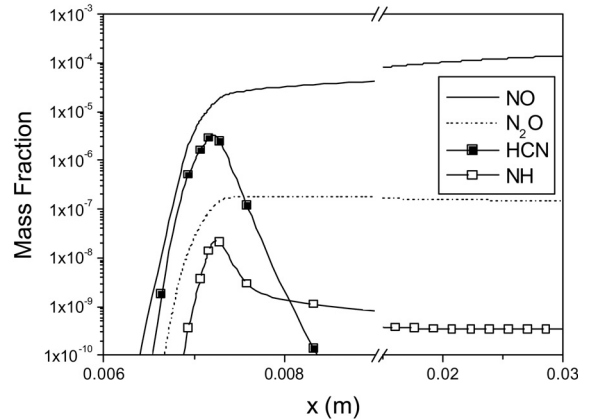

Fig. 2. Mass fractions of selected nitrogen compounds in the stoichiometric premixed methane–air flame.
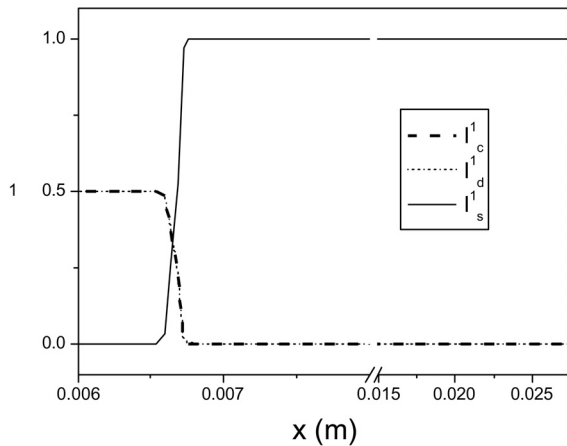
Fig. 3. The indices I_c^i, I_d^i and I_s^i for the 1st (i = 1) mode along the stoichiometric premixed methane–air flame.
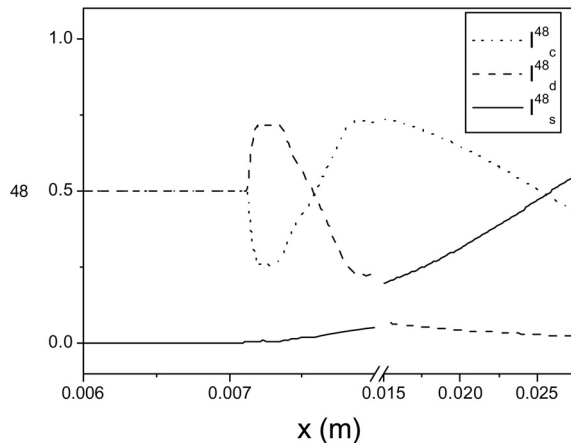

Fig. 4. The indices I_c^i, I_d^i and I_s^i for the 48th (i = N − E) mode along the stoichiometric premixed methane–air flame.

chemistry, as the dominant mechanism, takes place gradually. It starts right in front of the flame, where transport has accumulated enough radicals for the fuel to break-up, with the fastest chemical time scales overtaking the influence of transport and establishing chemical equilibrium in the phase-space directions along which they act. The transition then progresses, through the flame and the post-flame region, with the slower chemical time scales taking suit, until full chemical equilibrium is established. This is demonstrated in Figs. 3 and 4, where the indices I_c^i, I_d^i and I_s^i for the fastest (i = 1) and slowest (i = N − E = 48) modes are displayed. In both modes, convection balances diffusion in the preheat zone, with the action of chemistry being negligible. In the fastest mode chemistry starts

dominating right in front of the flame by establishing equilibrium, while in the slowest mode its dominance follows a much slower process, the action of transport (mainly convection) persisting far downstream.

At each point in the flame, the decomposition of the governing Eq. (1) in the form of Eq. (2) is meaningful only for the fastest modes, in which chemistry is dominating or is at least of equal importance to transport. However, inspection of the slower modes, in which chemistry is of secondary importance, reveals the formation of the kinetics components that will eventually further downstream drive these modes to equilibrium.

4. NO$_x$ formation mechanisms

NO is identified as the species affected by the slowest 48th mode (CSP radical) throughout the flame. The CSP radicals associated with the next five slowest modes, i.e. 47th to 43rd, include N_2O and HCN, the remaining three CSP radicals being major C-O-H species.

The indices I_c^i, I_d^i and I_s^i indicate that the mode associated with N_2O is dominated by transport in flame locations A and B (shown in Fig. 1), with chemistry starting to become important in location C and dominating in locations D to F. In addition, the indices J_k^i, reveal that the chemical time scale by which this mode is driven to equilibrium, throughout the flame, is specified by the reaction:

$$N_2O + H \Rightarrow N_2 + OH \tag{R183}$$

This reaction is the major consumption path for the nitrous oxide mechanism [6], tending to equilibrate reaction $N_2 + O + M \Rightarrow N_2O + M$ (−R185), as soon as a sufficient oxyhydrogen pool has been formed. Its influence to determine the chemical time scale to equilibrium is observed not only in points C to F, where chemistry is active, but also in points A to B, where chemistry is dormant.

The mode associated with HCN is dominated by transport in points A to C, with chemistry becoming important in point D and dominating in points E and F. The time scale by which this mode is driven to equilibrium is mainly specified everywhere across the flame by the reactions:

$$HCN + O \Rightarrow NCO + H \tag{R231}$$
$$HCN + O \Rightarrow NH + CO \tag{R232}$$
$$HCN + O \Rightarrow CN + OH \tag{R233}$$

the effect of (R231) being about three times larger than the combined effect of (R232) and (R233). These reactions form the second step of the prompt mechanism [6], initiated by reaction $CH + N_2 \Rightarrow HCN + N$ (R240).

CSP data show that the species N is associated with an extremely fast time scale and is always in steady state. Therefore, the HCN consuming reactions (R231–3) constitute the slow (rate limiting) component of the prompt mechanism and determine the related time scale.

The chemical time scale to equilibrium of the slowest mode, for which the CSP radical is NO, is mainly determined by reactions:

$$NH + NO \Rightarrow N_2O + H \tag{R199}$$

$$N + NO \Rightarrow N_2 + O \tag{R178}$$

Reaction (R199) dominates in points A to C, where the N_2O and prompt mechanisms are active, expressing an additional (but of minor importance) route to their equilibration [6]. On the other hand, reaction (R178) dominates in points D to F, where the N_2O and prompt mechanisms are equilibrated and the thermal mechanism is the only one interacting with transport.

5. Conclusions

Examination of the domain where the modes related to N_2O, HCN and NO are active and interact with transport and of the elementary reactions which determine the related chemical time scales, has revealed the emergence of the different NO_x-mechanisms in the various flame domains and the reasons for their equilibration.

It was shown that the chemical time scale for the equilibration of the N_2O, prompt and thermal mechanisms depends mainly on the levels of H, O and N respectively, radicals. Therefore, the first two mechanisms equilibrate in the main reaction zone, while the third equilibrates very far downstream. The associated time scales to equilibrium are among the slowest, compared to those emerging in the methane–air flame, the ones of the N_2O and prompt mechanisms being significantly faster than that of the thermal mechanism.

References

[1] Lam SH, Goussis DA. Conventional asymptotics and computational singular perturbation for simplified kinetics modeling. In: MO Smooke, editor. Reduced Kinetic Mechanisms and Asymptotic Approximations for Methane–Air Flames. Berlin: Springer Lecture Notes, 1991.

[2] Valorani M, Najm HN, Goussis DA. CSP analysis of a transient flame vortex interaction: time scales and manifolds. Combust Flame 2003;134:35–53.

[3] Rogg B. A computer program for the simulation of one-dimensional chemically reacting flows. Report CUED/A-THERMO/TR39, Cambridge University, 1991.

[4] Smith, GP, Golden DM, Frenklach M, Moriarty NW, Eiteneer B, Goldenberg M, Bowman CT, Hanson RK, Song S, Gardiner Jr WC, Lissianski VV, Qin Z. The GRI-3.0 Detailed Mechanism, http://www.me.berkeley.edu/gri_mech/.

[5] Peters N, Williams FA. The asymptotic structure of stoichiometric methane–air flame. Combust Flame 1987;68:185–207.

[6] Miller JA, Bowman CT. Mechanism and modeling of nitrogen chemistry in combustion. Prog Energy Combust Sci 1989;15:287–335.